Technical Report
TR-21-12
September 2021

Residual water and gases in a KBS-3 canister and their effect on post-closure safety

Kastriot Spahiu

SVENSK KÄRNBRÄNSLEHANTERING AB

SWEDISH NUCLEAR FUEL
AND WASTE MANAGEMENT CO

Box 3091, SE-169 03 Solna
Phone +46 8 459 84 00
skb.se

SVENSK KÄRNBRÄNSLEHANTERING

ISSN 1404-0344
SKB TR-21-12
ID 1952991

September 2021

Residual water and gases in a KBS-3 canister and their effect on post-closure safety

Kastriot Spahiu, Svensk Kärnbränslehantering AB

Keywords: Residual water and gases, KBS-3 canister, Damaged fuel, Radiolysis, Chemisorbed water.

This report is published on www.skb.se

Abstract

In this report some issues which need to be considered when formulating requirements for the allowed amount of residual water and air in a sealed KBS-3 canister are summarized. Water and gases that remain in an intact canister can cause a pressure increase in the canister and can also cause damage to the canister materials or to the spent fuel with damaged cladding through various processes. These include the production of potentially aggressive species such as HNO_3, NH_3 and H_2O_2 from the radiolysis of Ar-air-water vapour mixtures. In the first part of the report the consequences of 600 g residual water and 10 % or 1 % air are discussed from the point of view of their long-term effect on fuel with breached cladding and on the canister material. The discussion is based on the results of recent modelling studies of radiolysis of humid air in the canister atmosphere.

The second part of the report answers the question: How much water can be expected to be present in a sealed KBS-3 canister? The answer is based on a review of literature data for physisorption and chemisorption of water on all surfaces present in the canister and in the damaged fuel rods dried by industrial drying methods combining vacuum and high temperature. Based on these estimations of residual water in a canister load, which varies with the number of damaged dried fuel rods loaded, and on the results of the modelling of the processes in the canister interior, the long-term consequences for the fuel and canister materials are discussed for a few selected cases.

Sammanfattning

I denna rapport sammanfattas några frågor som måste övervägas när man formulerar krav på tillåten mängd restvatten och luft i en försluten kopparkapsel för använt bränsle. Vatten och gaser som finns kvar i en intakt kapsel kan orsaka tryckökning i kapseln och kan också orsaka skador på kapselns material eller på använt bränsle med skadad kapsling genom olika processer. Dessa inkluderar produktion av potentiellt aggressiva ämnen såsom HNO_3, NH_3 och H_2O_2 från radiolys av gaser och vätskor i kapseln. I den första delen av rapporten diskuteras konsekvenserna av 600 g restvatten och 10 % eller 1 % luft utifrån deras möjliga långsiktiga effekter på bränsle och kapselmaterial. Diskussionen genomförs baserat på resultaten av nyligen gjorda modelleringsstudier av radiolys av fuktig luft i kapselatmosfären.

Den andra delen av rapporten svarar på frågan: Hur mycket vatten kan förväntas finnas i en försluten kopparkapsel? Svaret är baserat på en genomgång av litteraturdata för fysisorption och kemisorption av vatten på alla ytor som finns i kapseln och i de skadade och torkade med industriella torkmetoder bränslestavarna. Uppskattningar av restvatten i en fylld kapsel varierar med antalet skadade bränslestavar i kapseln, samt på resultaten av modelleringen av processerna i kapselns inre. Baserat på dessa uppskattningar och resultat diskuteras de långsiktiga konsekvenserna för bränsle- och kapselmaterialen i några utvalda fall.

Contents

1 Introduction

In this report some issues which need to be considered when formulating requirements for the allowed amount of water and air in a sealed KBS-3 canister are summarized. Water and gases that remain in an intact canister can cause a pressure increase in the canister (Lilja 2012a) and can also cause damage to the canister material or to the spent fuel through various processes (e.g. radiolysis). SKB has analysed the issue of residual water and gases mainly with respect to the canister material.

Since a long time ago (SKB 2006), an upper limit of 600 g water has been accepted for a sealed canister. This upper limit is not the result of an analysis of the maximal amount of water which could be allowed without creating problems for the function of the canister or of the fuel, but is based on pessimistic assumptions about the number of damaged fuel rods which can be present in a canister load and their water content. Namely, it was assumed that 1 % of the fuel rods are damaged. With this assumption, there would be 12 damaged fuel rods (e.g. one in each fuel element with ~100 rods) in a BWR canister. Assuming the free volume in a fuel rod is 50 ml the total water volume would be 12×50 ml = 600 ml or 600 g. Both the assumption about the frequency of fuel rod cladding damages and the free volume in a fuel rod will be revisited in the second part of this report, when discussing the amount of water expected to be really present in a canister assumed to contain damaged fuel rods (packaged in separate containers or directly in the canister).

The objective in drying commercial LWR (Light Water Reactor) SNF (Spent Nuclear Fuel) containers is to eliminate enough water to preclude "gross" damage to commercial fuel or its cladding during transport and later in the deposition hole in the repository. Potential effects of residual water include degradation of spent fuel cladding, oxidation of exposed fuel pellets and potential corrosion of internal components in the canister. Especially problematic would be the oxidation of the exposed fuel pellets to U_3O_8(s), accompanied with a 36 % volume increase, which could cause cladding rupture and release of fuel particles in the canister. Finally, if the oxygen produced by water radiolysis is not consumed through oxidation of different materials, and radiolytic or metal corrosion hydrogen is produced, the gas mixture in the canister may be flammable, if a source of ignition is present (Jung et al. 2013).

The residual water in a canister is consumed in two major ways: through vapor radiolysis by the strong radiation field of the spent fuel with the production of H_2 and O_2 and through its reaction with the cast iron or carbon steel of the insert with production of magnetite as corrosion product and hydrogen gas. It is clear that if the process of reaction with iron is much faster than the radiolysis, the majority of water will be consumed by iron corrosion and only a small part will undergo radiolysis. The corrosion of structural parts of the fuel assemblies occurs also, but at much lower rates than the two above processes and has not been discussed in this report. Both processes occur simultaneously and only an elaborate modelling of both these processes, together with the process of fuel or copper oxidation by the radiolytic oxygen would make it possible to fully evaluate the consequences of the residual water. In this report the results of the modelling of the radiolysis of humid air (Henshaw and Spahiu 2021) in the canister, including the effect of the oxic and anoxic corrosion of iron will be discussed, as well as the results of the modelling of the effect of hydrogen produced by anaerobic iron corrosion on water vapour radiolysis (Jonsson 2021).

The different forms of water that can be found in a sealed canister are free or unbound water, physically adsorbed (or physisorbed) water and chemically adsorbed (or chemisorbed) water. Adsorption is the adhesion of atoms, ions or molecules from a gas, liquid or dissolved solid to a surface. This process creates a film of the adsorbate on the surface of the absorbent. The adsorption is a consequence of surface energy. In a bulk material, all the bonding requirements (be they ionic, covalent or metallic) of the constituent atoms of the material are satisfied by other atoms in the material. However, atoms on the surface of the adsorbent are not wholly surrounded by other absorbent atoms and can therefore attract adsorbates. The exact nature of the bonding depends on the details of the species involved, but the adsorption process is generally classified as physisorption when binding forces are characteristic Van der Waals forces and as chemisorption when the binding forces are chemical bonds. More information on the interaction of water with solid surfaces can be found in the reviews of Thiel and Madey (1987) and Henderson (1992).

For any process to occur spontaneously, the Gibbs free energy should be negative:

$\Delta G = \Delta H - T\,\Delta S$

The entropy change ΔS during adsorption is negative, since the adsorbate molecules pass from a more disordered state to a bound on the surface state. In general, solids which have high enthalpies of formation display also strong adsorption. In this report physisorption of water on metal surfaces such as copper or iron in the canister insert or metallic alloys such as stainless steel or zircalloy will be discussed. Most of the metals considered, such as iron or copper, have a thin layer of oxide on the surface, which makes the attraction forces less strong than in the case of metal atoms. According to Lee and Staehle (1997), this is the reason why less physisorbed water is found on iron or copper surfaces, as compared to gold.

The structure of the remaining text follows the requirements expressed for this report[1]. In the first part, the consequences of the presence of 600 g water in the canister for the canister material and the damaged fuel will be presented. In the discussion of the consequences for spent fuel, the special case of damaged spent fuel rods dried and packaged in Studsvik containers or Quivers under inert gas atmosphere will be discussed separately. In the second part of this report an analysis of a realistic amount of water expected to be present in the canister considering different scenarios for fuel drying and packaging is presented.

[1] Evins L Z, Lilja C, Olsson Å, 2020. Frågeställningar kopplade till frågor som rör gas eller vätskor inuti kapseln. SKBdoc 1890273 ver 1.0, Svensk Kärnbränslehantering AB. (In Swedish.) (Internal document.)

2 Consequences of 600 g residual water for the canister and the fuel

2.1 Consequences of 600 g residual water for the copper canister

The issue “Is 600 g water acceptable for the copper canister” has been discussed in the Fuel and Canister Process Report (SKB 2010a) and in a reply to a request for complementing information from SSM (Johansson and Neretnieks 2014).

In the section “Residual gas radiolysis” of the Fuel and Canister Process Report for SR-Site (SKB 2010a), the formation of nitric acid from the radiolysis of air and water vapour is discussed. It is demonstrated that a maximum amount of 450 g nitric acid can be formed, based on the maximum amount of nitrogen from the residual air in the canister. This amount of acid will cause the corrosion of a 10 µm layer of the cast iron insert. The consequences of the presence of nitrate ions on stress corrosion cracking of the insert are discussed by Lilja (2012b) showing that they are negligible.

In a request for complementing information from SSM (SSM 2012, question 6), the question of the damage on the copper canister caused by the radiolysis of all the amount of water collected at the bottom of the canister in the gap between the copper shell and the insert, where the temperature is expected to be lower, was raised by the authorities. The reply of SKB (Johansson and Neretnieks 2014) considered various situations, including the collection of 600 g water as liquid at the bottom of the canister between the insert and the copper shell. The amount of water vapour that undergoes radiolysis until all Cs-137 decays in the gap between the canister and the insert is estimated as 0.5 g and the oxidants produced are expected to corrode 14 µm copper, spread over all the inner copper surface. If all the water is condensed at the bottom of the canister in the gap between the insert and the copper shell in a column 134 mm high, the amount of radiolysed water after 1 000 years is 45 g. Assuming that all the oxidants produced react with copper, they would cause a corrosion depth of 0.07 mm. If the effect of gradually disappearing water because of iron corrosion is accounted for, the lowest part of the 134 mm height might corrode to twice that depth. Finally, the oxidizing effect of volatile fission products such as Cl and I originating from breached fuel rods is estimated. They could at most oxidize 0.08 mol copper to Cu(I), but it is most likely that they react with iron before reaching the copper. It was thus concluded that the limit of 600 g water was acceptable for the copper canister. The recent modelling results (Henshaw and Spahiu 2021) modify slightly this conclusion, as will be discussed in the next section.

2.2 Radiolysis of humid air and iron corrosion inside a KBS-3 canister

The amount of nitric acid in the Fuel and Canister Process Report (SKB 2010a) was estimated from mass balance calculations based on the amount of nitrogen in residual air in the canister (10 % of the total free volume of 1 m^3 in a BWR canister (SKB 2010c), the rest being Ar) as 450 g HNO_3. The estimation was based also on the modelling work of Henshaw et al. (1990) and Henshaw (1994), carried out for the Advanced Cold Process Canister (ACPC) with relatively low amounts of water (50 g) and air (< 1,7 %) as compared to the current requirements (maximum 600 g water and 10 % air in the sealed canister). For this reason, a modelling of the processes occurring in a sealed KBS-3 canister during the initial 500 years, when the γ-field of the fuel causes radiolysis of the humid air, was carried out recently for the relevant conditions (Henshaw and Spahiu 2021). The results of the modelling for 600 g water and 10 % air, neglecting any contribution of iron corrosion, show that the total amount of nitric acid produced is about 0.83 moles (~ 52 g), i.e. about 9 times lower than the amount estimated through mass balance calculations (SKB 2010a). There are also 2.2 mol H_2O_2, 0.06 mol O_2 and 3.2 mol H_2 produced by radiolysis.

When the simultaneously occurring corrosion of iron surfaces is considered, several new features appear, which will be discussed further here. There is a large surface of carbon steel (fuel channel walls) and cast iron in the insert (35 m^2, SKB 2010b) which is in contact with residual water. Water is mainly in the vapour form, especially during the first two years when the temperature in the

canister is high. In the presence of oxygen (originating from 10 % residual air), oxic corrosion of iron occurs. The corrosion product is usually γ-FeOOH at room temperature and the reaction is:

$4Fe + 2H_2O + 3O_2 = 4\ FeOOH$

where FeOOH represents goethite (α-FeOOH) or lepidocrocite (γ-FeOOH). Crystallization of the initially formed amorphous ferrioxyhydroxide may also occur, resulting in formation of maghemite (γ-Fe_2O_3) or hematite (α-Fe_2O_3). As initially present oxygen is consumed, Fe(III) corrosion products will be transformed to magnetite, either by reaction with dissolved Fe(II) or by reductive dissolution coupled to iron dissolution. Increasing the temperature to 50–100 °C favours the formation of Fe_3O_4, since at temperatures around 100 °C, $Fe(OH)_2$ decomposes to Fe_3O_4+H_2.

The uniform oxic iron corrosion rate is also a function of temperature (Uhlig and Revie 1985). Increasing the temperature causes a linear increase in the corrosion rate of iron in water. Beyond 75 °C, the corrosion rate in an open system decreases in the temperature range 75–100 °C. This is a result of the decreased solubility of oxygen in solution as the temperature is increased. On the other hand, in a closed system such as the canister, where the oxygen concentration is not allowed to decrease, the corrosion rate continues to increase with temperature.

Constant corrosion rates of 0.4 or 0.2 mm/y were chosen by Henshaw and Spahiu (2021) for this reaction, based on the work of Swanton et al. (2015) (see their Fig. 4), Sridhar et al. (1994), Speller (1951) and Uhlig and Revie (1985). The value of 0.4 mm/y corresponds to 70 °C and, given that the duration of this corrosion mode is only a few hours, higher temperatures and higher corrosion rates were not tested. Instead, a lower corrosion rate of 0.2 mm/y, typical for room temperature corrosion of carbon steel in aerated water was also tested (Henshaw and Spahiu 2021).

The anoxic corrosion of iron starts when all initial oxygen is consumed according to:

$3\ Fe + 4\ H_2O = Fe_3O_4 + 4\ H_2$

The most important parameter for evaluating the rate of water consumption and hydrogen production through insert material corrosion is the corrosion rate of carbon steel or cast iron with water vapour at the given conditions. The corrosion rate under anoxic conditions is also independent to whether water is present as liquid or as vapour (Smart et al. 2002). The presence of radiation increases markedly the corrosion rate of iron, as shown in the tests reported by Smart and Rance (2005) and Puranen et al. (2017). Corrosion rates of 3 μm/year are reported by Smart and Rance (2005) for cast iron corrosion in modified Allard groundwater at 30 °C in the presence of 300 Gray/h γ-radiation, which showed no sign of decrease during the ~416-day duration of their test. Puranen et al. (2017) measured higher rate of hydrogen production during iron corrosion in the presence of spent fuel than in its absence during more than 3 years, without any sign of rate decrease. With a corrosion rate of 3 μm/year and 35 m^2 surface of the insert (SKB 2010b), a volume of 105 cm^3 Fe is corroded each year. With carbon steel density of 7.85 g/cm^3 this corresponds to 824 g Fe or 14.76 mol Fe. This would consume 19.7 mol H_2O (from $3Fe + 4H_2O = Fe_3O_4 + 4H_2$), which corresponds to 354 g H_2O and would produce 19.7 mol H_2, i.e. the hydrogen production rate in the canister is 0.054 mol/day. With this iron corrosion rate by water vapour, the 600 g water would be consumed during 1.69 years in the canister. The presence of initial oxic corrosion shortens this period to 1.6 years (Henshaw and Spahiu 2021).

It should be considered that when analysing the corrosion inside the canister, initial anoxic corrosion rates are relevant and they are usually higher than long term corrosion rates (see e.g. Fig.12 and 13 in Swanton et al. (2015)).

The modelling results of Henshaw and Spahiu (2021) show that when considering iron corrosion as described above, nitric acid is produced during the first 10 h after canister sealing, while O_2 is still present in the system, but then starts to decrease as both O_2 and H_2O_2 are consumed. O_2 is consumed via oxic iron corrosion, while H_2O_2 is consumed as H_2 starts to be produced from anaerobic iron corrosion. The gas phase radiolysis reactions will reform H_2O from H_2O_2 and H_2, which is subsequently lost via anaerobic corrosion.

With the loss of O_2 from the system, NH_3 starts to form until steady state concentrations of H_2 and NH_3 are achieved. The amount of nitric acid produced in this case is very small (~0.23 mg) and in the presence of ammonia, it would probably form NH_4NO_3. Other oxidants (O_2, H_2O_2) have negligible levels ($< 2 \times 10^{-12}$ mol). Ammonia is produced due to the radiolysis of H_2 (produced by anoxic iron corrosion and water radiolysis) and N_2 (from residual air) mixtures in the canister interior under anoxic conditions and when ammonia reaches its peak (~1.3 mol), all water is already consumed by corrosion. The use of lower oxic corrosion rates (0.2 mm/y, relevant for room temperature oxic iron corrosion) results in the production of ~0.4 mg HNO_3 due to the slower removal of oxygen from the system, otherwise this case is quite similar to the one with an oxic corrosion rate relevant for 70 °C. As discussed in Henshaw and Spahiu (2021), with 600 g residual water there is a short period of approximately 150 days (between 10^3 and 10^4 hours) after canister sealing when both ammonia and water exist in the system. Ammonia can potentially lead to altered corrosion mechanisms of the canister materials, anyhow the ammonia amounts in the canister when water is present are relatively low (< 7 g, i.e. the gas phase NH_3 concentration is 7 mg/l).

The results of the calculations with 600 g residual water and 1 % air, without considering corrosion, show that only 3.6 g HNO_3 is produced as compared to 52 g in the presence of 10 % air. Other radiolysis products formed in the canister in this case are 1.4 mol H_2O_2, 0.12 mol O_2 and 1.7 mol H_2. Thus, by lowering the residual air 10 times lowers the amount of nitric acid almost 15 times, and this improvement in the canister atmosphere is very desirable.

When corrosion is considered in the case of 600 g water and 1 % air, negligibly small amounts of oxidants such as nitric acid (~2 µg), H_2O_2 (~2×10^{-14} g) and O_2 (1×10^{-15} g) are formed by radiolysis, together with 0.13 mol ammonia. The difference with the 10 % air case is that all water is already consumed when ammonia starts to form, i.e. there is no period in which water and ammonia coexist.

2.3 Consequences of 600 g residual water for damaged fuel

The spent fuel is the waste form, and criteria about acceptable conditions in the sealed canister can be formulated only in relation to its further behaviour as the source term in the repository.

It is self-evident that in canisters where all the fuel rods have undamaged zircalloy cladding or in these canisters which contain fuel packaged in stainless steel containers (Studsvik or Quiver) with dried fuel in inert gas atmosphere, the influence of the humidity outside the fuel rods does not need to be considered. It is assumed that a canister load with all fuel rods undamaged can be dried appropriately and the only water remaining in the canister is physisorbed water on the copper shell, and possibly on the canister insert and the fuel elements resorbed during transport after drying, see Section 3.1.

The issue of water presence becomes relevant if the known damaged fuel rods present in Clab (251 rods, out of which 197 are certain)[2] and the few (4 to 6 in total) rods which may have been damaged during storage in Clab (detection of Kr-85 in the ventilation system) are packaged in the presence of 600 g water. This assumption is both not realistic and over pessimistic, because the assumed amount of water depends on the number of damaged fuel rods and the maximum amount of water possible to be contained in a damaged fuel rod, see further Section 3.2. The number of completely water-logged old design fuel rods needed to contain 600 g water would be 15 in a canister load and the number of dried fuel rods with 4 g residual water (see Chapter 3) would be 150.

The water present in the canister will be mostly in vapour form, especially in the first 10 years when the temperature in the canister is relatively high. The highest temperature is on the surface of the fuel rods, reaching up to 140 °C during the first decade in some canisters, see Figure 2-1.

[2] Huuva E, 2021. Läckande bränsle i Clab bassänger. SKBdoc 1911213 ver. 1.0, Svensk Kärnbränslehantering AB. (In Swedish.) (Internal document.)

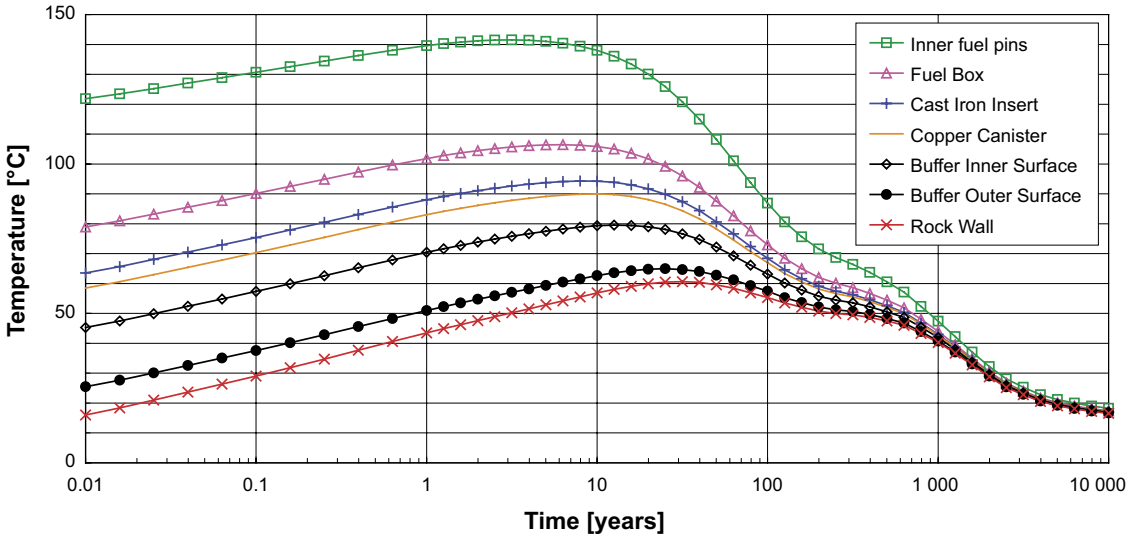

Figure 2-1. *Temperature evolution in a canister (SKB 2006, Fig. 9-17).*

In order to estimate the effect of residual water on breached fuel rods, a modelling of the radiolysis of water vapour is necessary. Then a modelling of the oxidation of breached fuel rods at the expected temperatures, including estimations of the exposed fuel surface has to be carried out as it is done e.g. in Jung et al. (2013) and Shukla et al. (2019). If necessary, the oxidation of the zircalloy cladding may also be considered. The water vapour will be affected by γ-radiolysis caused by the radiation of the spent fuel, and in the exposed fuel surfaces alpha radiolysis of steam will also be operative. At the same time, water vapour reacts with the iron insert and produces hydrogen, which affects all types of water vapour radiolysis.

Some issues concerning fuel oxidation, based mainly on the works of Jung et al. (2013) and Shukla et al. (2019), as well as other literature sources will be discussed. It should be mentioned that requirements concerning cover gases in dry fuel storage casks specify no more than 0.2 % oxidizing species in the gas atmosphere (Knoll and Gilbert 1987). From this point of view, the allowed maximum presence of 10 % air (i.e. ~2.1 % oxygen) in the KBS-3 canister gas atmosphere is a relatively high level. This is why calculations with lower residual air, 1 %, were carried out recently (Henshaw and Spahiu 2021).

Jung et al. (2013) use a simplified radiolytic model in which water is assumed to be decomposed by radiolysis to O_2 and H_2. G-values are typically used to estimate the rate of production of radiolytic species or the molecular decomposition as a result of ionizing radiation. The G-values used were taken from Arkhipov et al. (2007), including a G-value for water decomposition G_{H2O} = 7.4 particles/100 eV. Then two values for the rate of energy deposition (dose rate), which cover the whole space in the canister are calculated based on the type and amounts of spent fuel. The decomposition of water $2H_2O = 2H_2 + O_2$ occurs within 4.77 years or 71.62 years respectively for the low and high dose rates. The oxygen produced through radiolysis participates in the oxidation of the spent fuel and that of the cladding, even though the results show that the oxidation of zircalloy is negligible.

The spent fuel is assumed to be oxidized to U_4O_{9+x} (usually up to $UO_{2.4}$) at temperatures below 230–250 °C and relative humidity below 40 %, based on the data of Hanson (1998), Einziger et al. (1992), Thomas et al. (1989, 1993), see Figure 2-2.

At the temperatures expected in the canister (maximum 140 °C at the surface of the fuel) the oxidation of fuel does not go beyond $UO_{2.4}$ (Hanson 1998, Thomas et al. 1993). This is due to the increased stability of the cubic structure of U_4O_9(s) by the presence of the fission products, and the oxidation proceeds to U_4O_{9+x} (usually up to $UO_{2.4}$). The formation of a U_3O_7(s) phase, typical during oxidation of uranium dioxide in air, is not observed for spent fuel (Hanson 1998, Thomas et al. 1993). Temperatures higher than 230 °C are needed to form U_3O_8(s) (Einziger and Cook 1985, Einziger and Strain 1986), see Figure 2-2. This transformation is accompanied with a large volume increase (36 %) due to the passage from a cubic to a tetragonal phase (Taylor et al. 1989), and can cause cladding rupture due to fuel swelling (unzipping).

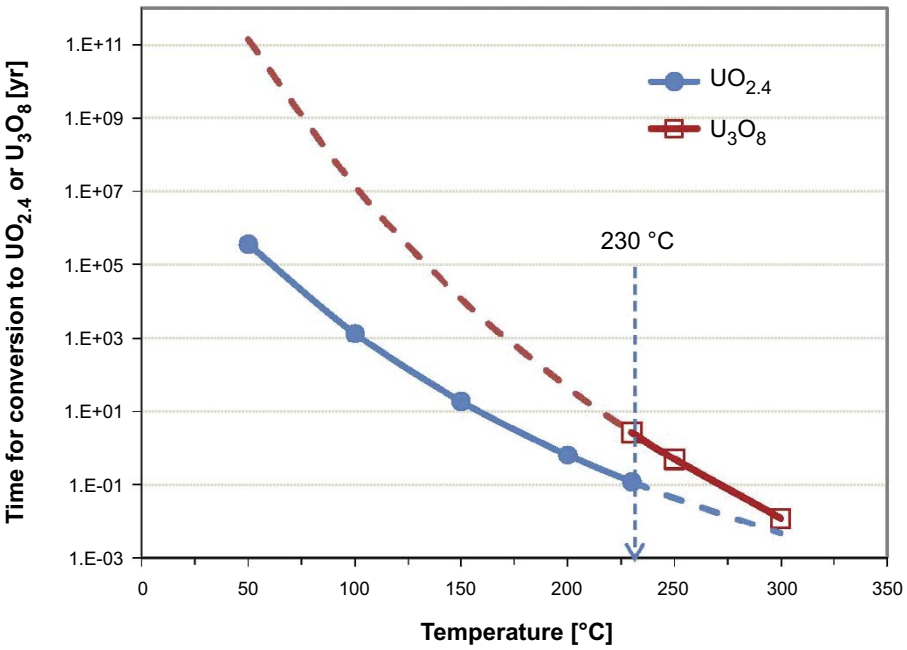

Figure 2-2. *Time for conversion from UO_2 to $UO_{2.4}$ and from UO_2 to U_3O_8 as a function of temperature (from Jung et al. 2013).*

For temperatures below 150 °C, spent fuel is oxidized to $UO_{2.4}$ for relative humidity below 40 % and to $UO_3 \cdot xH_2O$, x = 0.5–2, for higher relative humidity (Taylor et al. 1989, 1995, Wasyvich et al. 1993) or in water solutions. The formation of $UO_3 \cdot xH_2O$ during oxidation of fuel in the presence of humid air is reported mainly based on UO_2(s) oxidation studies or oxidation of Candu fuel with relatively low burnup. A later study with LWR fuel in water saturated atmosphere at ambient temperature (Leenaers et al. 2003) reports formation of U_4O_9 both in dry and in humid atmosphere.

Certain differences on fuel oxidation are reported in Shukla et al. (2019), as compared to Jung et al. (2013). The temperature limit for oxidation of low burnup fuel to U_3O_8 is raised to 250 °C, over which U_3O_8 is formed at measurable rates. Further, a burnup dependence of fuel oxidation is introduced based on the studies of Kansa et al. (1999), which have determined an incubation period for the oxidation to U_3O_8 increasing with burnup.

Anyhow the result will be that the already partially oxidized fuel of the damaged rod will be further oxidized by radiolytically produced oxygen. In the first version of this report[3], in absence of modelling results for the processes occurring in the canister, only mass balance calculations could be used to estimate an upper limit of the oxidized fuel. This resulted in a total 50.5 mol UO_2 (13.63 kg fuel) that can be converted from UO_2 to $UO_{2.4}$, if all water is radiolysed only to hydrogen and oxygen and all the produced oxygen is assumed to react with the fuel. It should be considered that one mol H_2O produces 0.5 mol O_2 and one mol O_2 oxidizes 5 moles UO_2 to $UO_{2.4}$ and 2 moles UO_2 to $UO_3 \cdot xH_2O$. The kinetics of fuel oxidation to $UO_{2.4}$ depends on the temperature and it would take e.g. 1310 years at 100 °C (Jung et al. 2013) and 30.7 years at 140 °C (see Section 3.2). This is an extreme upper limit that would require the presence of the corresponding amount of damaged fuel in the canister, e.g. 7 damaged BWR fuel rods with ~2 kg fuel each in the same canister.

Further, the modelling of the radiolytic water decomposition and fuel oxidation in Jung et al. (2013) and Shukla et al. (2019) shows that a very small fraction of the fuel in the damaged rod present in their dry storage canisters is in fact oxidized. Jung et al. (2013) consider fuel oxidation in a Castor 21 cask containing 4368 fuel rods, out of which 4 are damaged, in the presence of 100 g or 1000 g water. The damaged fuel rods are assumed distributed one in each temperature zone in the canister and zone 4, with temperatures 152–250 °C is the one nearest to the temperatures in the KBS-3 canister

[3] Spahiu K, 2020. Residual water in a KBS-3 canister and its effect on post-closure safety. SKBdoc 1914189 ver.1.0, Svensk Kärnbränslehantering AB. (Internal document.)

(the fifth zone, with even lower T, has no damaged fuel rod). The amount of fuel oxidized to $UO_{2.4}$ in the presence 100 g water is 10 g in zone 4 and 59.2 g in all the four zones, while in presence of 1000 g water the amount of fuel oxidized to $UO_{2.4}$ in the four damaged rods is 86.9 g, i.e. about 1 % of the total fuel mass in the 4 damaged fuel rods. This is mainly due to the fact that a very small part of the damaged fuel rod is oxidized by oxygen at high temperature, based on the experimental results of Einziger and Cook (1985). Their tests show that only ~3 cm of the fuel rod on both sides of the defect was oxidized at 230 °C, the rest of the rod was unaffected.

To evaluate the consequences of residual water in a KBS-3 canister means to consider the long-term radiolytic decomposition of water into hydrogen and oxygen, the oxidation of the exposed surface of the fuel rod to U_4O_9(s) by radiolytic oxygen at 140 °C, as well as the potential oxidation of the zircalloy cladding. Given the relatively high temperature in the canister, all this water (unbound and physisorbed) will be in vapour phase and the small amounts of water expected to be present (see Chapter 3) will contribute a relative humidity inside the canister well below 40 %. Given that the temperature in the KBS-3 canister never reaches 230–250 °C, the oxidation of UO_2 to U_3O_8(s) and the accompanying volume increase, which can cause severe damage to the fuel, can be excluded. The amount of fuel which can be oxidized to U_4O_9(s) will depend on the kinetics of the oxidation and at the temperatures in the canister. The time to oxidize fuel from UO_2 to $UO_{2.4}$ at 140 °C, can be calculated using the expression reported by Hanson et al. (2008):

$$t_{2.4}(h) = 1.40 \times 10^{-8} \exp (105\ kJ/RT)$$

where $t_{2.4}$ (h) is the time in hours to oxidize UO_2 to $UO_{2.4}$, R is the universal gas constant and T temperature in Kelvin, results in 30.7 years if radiolytic oxygen is present so long in the canister void. The authors warn that the above expression is valid for LWR fuel and not for CANDU fuel, which has much lower burnup.

When contacted by groundwater in the case of a canister failure expected to happen much later, this pre-oxidized fuel will be dissolved with a higher rate than pristine fuel, until all the pre-oxidized uranium is released. Experimental studies and field observations with pre-oxidized uranium oxide (uraninite) leached under anoxic conditions in groundwaters and solutions containing U(VI) complexing agents such as bicarbonate, show that the pre-oxidized uranium is released and the matrix is converted to $UO_{2.00}$ (Rafalskiy et al. 1979). This was confirmed also in an experimental study where Gd-doped UO_2 was pre-oxidized at high temperature in an oven to $UO_{2.4}$ and then leached in carbonate solutions under anoxic conditions (Ollila and Lindqvist 2003). A gradual increase of the lattice parameter of the Gd-doped UO_2 was observed with leaching time, indicating that the solid releases the oxidized uranium and slowly converts to $UO_{2.00}$. After the pre-oxidized uranium is released during a given period with higher dissolution rates, the fuel is expected to behave as normal fuel afterwards.

SKB has made an evaluation of the dissolution rates of the altered fractions of fuel with damaged cladding and assumed relatively high dissolution rates (Evins and Hedin 2020). First, since it is not possible to evaluate how much fission products and actinides the damaged fuel has released from the damage in the reactor until it is placed in the canister after drying, the full inventory of this fuel rod will be used in the safety assessment. This is a pessimistic assumption, because higher release rates are assumed for the pre-oxidized part of this fuel and include also e.g. the instant release nuclides such as Cs and I, which for this fuel rod very probably have already been released and are deposited in the ion exchangers of Clab or nuclear power plants. Second, no credit is taken for the potential conversion of the fuel to $UO_{2.00}$ after the release of the pre-oxidized fraction of uranium, instead all of the altered layer (containing pre-oxidized uranium) is pessimistically considered to be dissolved with much higher rates.

Further, this amount of oxidized uranium in the canister is a hypothetical upper limit, because the mechanism causing the fuel oxidation is the radiolysis of water and all the radiolytic oxidants are assumed to be consumed only by the fuel. The water vapour will react simultaneously with the iron of the canister insert under anoxic conditions and produce hydrogen, as discussed in Section 2.2. Already in less than 3 months after canister sealing, the corrosion of iron of the canister insert by water vapour will produce enough hydrogen to constitute more than 10 % of the atmosphere inside the canister. This is expected to reduce considerably the production of oxidants by γ-radiolysis (Pastina et al. 1999, Pastina and LaVerne 2001), and in the presence of this amount of hydrogen in the canister atmosphere, the oxidant production by γ- radiolysis is expected to be quite low.

As mentioned before, a modelling of the γ-radiolysis of 600 g water vapour inside a sealed canister in the presence of the hydrogen produced by the corrosion of carbon steel and cast iron has been carried out (Jonsson 2021). The radiolytic reactions are the same as for liquid water (but with different values of the kinetic constants) and their temperature dependence is thoroughly investigated driven by the needs to model radiolysis in nuclear reactors (Bartels et al. 2013). The influence of the inert gas (Ar) participating in 3-body reactions was also investigated. The results show a very strong influence of hydrogen in the radiolysis of water vapour: the radiolytic oxidant (H_2O_2 and O_2) concentrations drop to negligible levels ($< 10^{-16}$ mol) for hydrogen amounts in the canister void higher than 3.3×10^{-3} moles. With a hydrogen production rate of 0.054 mol/day (Section 2.2), this is achieved in ~1.5 hours of anoxic iron corrosion.

Another issue which is not discussed in any other literature sources cited here is the potential effect of alpha radiolysis of water vapour in the atmosphere in the canister. Experimental data of alpha radiolysis of steam at high temperatures (Olander et al. 1997, 1999, Li and Olander 1999) indicate that the presence of 10 mol% hydrogen in the steam decreases considerably the radiolytic decomposition of water. In batch irradiation experiments reported in Li and Olander (1999), the yield of H_2O_2 could not be measured, but radiation produced O_2 was detectable. On adding H_2 to the steam, the G-value for O_2 decreased sharply; for 8.5 mol% H_2 in the steam at 70 atm, the O_2 yield in the steam was a factor 25 lower than the value in pure steam. The loss of O_2 could have resulted from reaction of this species with excess H_2 to produce hydrogen peroxide. However, none of this product was detected. It appears that the relatively small concentration of added H_2 essentially stops net water decomposition by efficiently converting O_2 and H_2O_2 back to H_2O.

These experimental data concern alpha radiolysis under nuclear reactor conditions, i.e. at higher temperatures than in the KBS-3 canister; however, the hydrogen concentrations expected in the canister quickly reach levels much higher than 10 mol% of the canister atmosphere.

Several other studies, carried out with actinide oxide surfaces in the presence of a few layers of adsorbed water have been reported in literature, indicating that actinide oxide surfaces cause recombination of radiolytic products back to water. The results of a radiolytic gas generation study on NpO_2(s) doped with 0.7 % ^{244}Cm in the presence of moisture contents up to 8 wt% water (Icenhour et al. 2004) show that radiolytic gas generation quickly reaches a steady state plateau at relatively low total pressures. The plateau is interpreted by the authors as clear evidence of a significant back reaction (i.e. the recombination of the radiolytic products O_2 and H_2 to water) where the rate of the forward reaction (radiolytic decomposition of water) is equal to that of the back reaction, a behaviour noticed by the authors also in other systems. Haschke et al. (1996) observed a pressure decrease in a 2:1 (D_2+O_2) gas mixture over $^{239}PuO_2$(s) at 25 ºC, which was interpreted as caused by the catalytic formation of water on the surface of PuO_2(s). The role of alpha radiation in the interfacial processes involved in both these studies has not been discussed in the original publications, but its influence cannot be excluded (Korzhavyi et al. 2004).

Finally, in long term radiolysis experiments (Cera et al. 2006, Cui et al. 2008, Eriksen et al. 2008) with spent fuel fragments in sealed glass ampules with 30 ml bicarbonate containing water under initially argon atmosphere, the production of radiolytic oxygen and hydrogen practically ceased after one year and the H_2 and O_2 levels were constant in ampules opened after 1, 2 or 3 years.

2.4 Summary on the consequences of 600 g residual water

The question that was posed in the beginning of this section was “Is 600 g water acceptable for the copper canister and for the fuel?”

Based on the recent modelling studies (Jonsson 2021) and (Henshaw and Spahiu 2021), the results of radiolysis calculations together with simultaneous corrosion of iron show that 600 g water is acceptable for the canister even in the presence of 10 % air, with the reservation that this involves a ~150 days period during the first 1.6 years with the coexistence of water and ammonia. Ammonia could potentially alter the corrosion behaviour of canister materials. There is no such reservation for 600 g water, if air can be kept below 1 %. In conclusion, 600 g water is acceptable for the canister, with no reservation if air is below 1 %.

The modelling shows that the amounts of oxidants (HNO_3, O_2, H_2O_2) produced by 600 g water, even in the presence of 10 % air, are very small (< 0.4 mg) and would oxidize a negligible part of fuel with breached cladding. Thus 600 g water is acceptable for the fuel too. No literature data could be found on any long-term effects of small amounts of dry ammonia (< 22 mg/l) present in the canister atmosphere for the fuel or the canister materials.

3 Estimation of residual water in a sealed KBS-3 canister

3.1 Case when all fuel rods have undamaged zircalloy cladding

In this case it is assumed that an industrial drying process (e.g. vacuum drying at high temperature, using FGD (Forced Gas Dehydration) or similar methods), including a pressure rebound test (control of the residual water pressure under 3 Torr during 30 min) has been carried out (ASTM 2016). In a report by Miller et al. (2013) the potential locations where residual water may remain after vacuum drying of canister for dry fuel storage are discussed. The designs of both BWR and PWR fuel assemblies were reviewed and locations where water could be trapped or difficult to remove during drying were identified. One important case is that of a rod with breached cladding, which will be discussed later in Section 3.2. Other locations identified are the dashpot region of the guide thimble tube for PWR assemblies and the water rod for BWR assemblies, which are hollow tubes where water can flow but which are closed at the bottom end. Finally, water could be difficult to remove from creviced regions around geometrically complex assembly hardware such as grids, nozzles and tie rods. The methods to measure residual water are also discussed in Miller et al. (2013), including experience from pharmaceutical industry. In another report (Knight et al. 2018) the results of drying experiments with a full-scale mock-up of a BWR or PWR fuel element are presented and a method for measuring low concentrations of water by emission spectroscopy (OES) is described. Freezing was detected at the bottom of the chamber due to inadequate heating of the bottom part and was remediated by adding heating tape and isolation to the bottom of the chamber. More than 120 drying tests were carried out with the chamber. In all tests, the assembly and chamber features were dried during normal industry procedures. The only exception was freezing at the bottom of the chamber and the case of the failed fuel rod, discussed in the next point here. Based on these data, it can be assumed that the fuel elements which do not contain damaged fuel rods and are dried under normal industry procedures do not contain any unbound water.

In the current design of the encapsulation plant, no drying of the copper canister is considered. This means that physisorbed water will exist at the inner surface of the copper shell and its amount will depend on the air temperature and relative humidity. The same holds for the canister insert, which does not undergo any drying procedure, except for filling with inert gas after the emplacement of the fuel elements.

An estimation of the amount of **physisorbed water** in the inner surface of the copper shell can be made from the total surface of 15.1 m^2 (SKB 2010b) and published data on water sorption on copper (Lee and Staehle 1997). The result is 46 mg water at 80 % RH (Relative Humidity) and 74 mg water at 100 % RH. The total amount of physisorbed water on the surface of the carbon steel or cast iron BWR insert with a surface of 35 m^2 (SKB 2010b) and water physisorption data for iron from Lee and Staehle (1997) will be 77 mg at 80 % RH and 86 mg at 100 % RH. As discussed in Lee and Staehle (1997), their data show multilayer sorption on the corresponding oxides formed on the surface of the metals and agree well with literature data, e.g. these of Seo et al. (1990) and Dante and Kelly (1993). In the case of a PWR canister insert with a total surface of 17 m^2 (SKB 2010b), the amount of physisorbed water in the insert will be 37 mg for RH 80 % and 42 mg at 100 % relative humidity. From the average temperature and relative humidity in Oskarshamn during one year, an estimation of the physisorbed water can thus be made.

The fuel elements will be dried appropriately before being placed in the canister insert and will be left there 24 hours before placing the lid of the insert. The transfer will be made in air and the possibility to physisorb water during the transfer exists, even though the fuel assemblies may be warm after drying and thus adsorb less water. For this reason, physisorbed water on the surfaces of fuel assemblies is accounted for in the estimation of the total amount of water in the sealed canister.

No data could be found in literature for physisorption of water on zircalloy as a function of relative humidity, apparently because atmospheric corrosion of zircalloy is not so relevant. On the other hand, several studies report the state of the adsorbed water on monoclinic ZrO_2. Hall and Langran-Goldsmith (1992) determined water adsorption on monoclinic ZrO_2 powder, with BET surface area of 1.9 m^2/g

and estimated 0.28 mg/m^2 for an adsorbed water monolayer. At 30 °C and 70 % RH, the amount of water adsorbed was 2.13 mg/m^2 of the solid surface. At high relative humidity, the data of Holmes et al. (1974) on adsorption/desorption of water on monoclinic ZrO_2 (see their Figure 3) correspond to adsorption of 3 mg/m^2. The hysteresis in the adsorption/desorption curve is due to the first chemisorbed layer of water, i.e. this value includes both physisorbed and chemisorbed water on zirconium oxide. Dellongueville et al. (2013) carried out TGA (Thermo Gravimetric Analysis) coupled with gas analysis and isotherm analysis at 150 °C of water adsorbed on a 26 µm thick corrosion layer of Zircalloy-4. The TGA data indicate that most of the water is released between 100 and 300 °C and only a small amount is released at higher temperatures. They conclude that a thermal treatment at 150 °C for 10 hours eliminates most of the water adsorbed on zircalloy.

The issue of **chemisorbed water** has been discussed in various publications (ASTM 2008, 2016, Jung et al. 2013, Shukla et al. 2019), but in none of them is undertaken any quantitative estimation of the amount of chemisorbed water. Chemisorbed water in the zircalloy cladding seems anyhow to be the basis for the upper limit of residual water used in Jung et al. (2013), see further Section 3.2. In the case of fuel with intact cladding discussed here, chemisorbed water is mentioned in connection with hydrated compounds of Zr of the cladding material. Chemisorbed water on uranium compounds will be discussed in the next section (3.3), while discussing damaged fuel rods.

In a review on zircalloy corrosion Gras (2014) states:"The corrosion kinetics of zirconium alloys in high temperature high pressure steam or water can be schematically described by a first "parabolic-type" regime, up to the so-called transition point, followed by a series of parabolic curves often approximated by a linear law. The transition is observed for an oxide layer of thickness in the range 2–3 µm and is correlated with a loss of the oxide protective character. Pre-transition oxide, of tetragonal structure, is a thin, nonporous, black oxide layer that grows in thickness with the cube root of time eventually transforming into the post-transition grey oxide layer. The post-transition grey oxide layer has some porosity; its structure is monoclinic. Thus, when a thick oxide is produced from reaction with water or steam, most of the oxide exists as the monoclinic zirconia".

In the NEA TDB review of Zr (Brown et al. 2005) the three polymorphs of crystalline ZrO_2(cr) with monoclinic, tetrahedral and cubic structures are discussed. The monoclinic phase is the one stable at low temperature and the monoclinic-tetragonal transition occurs at 1174 °C under 1 bar pressure (Alcock et al. 1976), while the tetragonal-cubic transition occurs at even higher temperatures. The thermal decomposition of low temperature amorphous gel-like precipitates formed in aqueous phases such as $ZrO_2 \cdot nH_2O$ or $Zr(OH)_4$ leads in many cases to the metastable formation of the tetragonal modification (Tosan 1991) which can be transformed irreversibly to the monoclinic phase at high temperature. The reasons invoked for the stabilisation of the tetragonal phase at low temperature include the effect of particle size on the Gibbs energy of formation (Garvie 1965, Holmes et al. 1972), the similarity of the Zr-O distances in the precipitated gel and in the tetramer phase formed by olation from the gel. Other reasons for the formation of the tetragonal crystalline phase are the high pressures experienced at the corrosion site in the reactor (Roy and David 1970). It seems thus that the layer of zirconia formed from the water corrosion of zircalloy in the reactor is composed of the tetragonal and monoclinic polymorphs of crystalline ZrO_2(s). Any initially formed amorphous phases under the high temperature and pressure conditions in reactor give rise to the tetragonal phase, which later continues to grow as the monoclinic phase.

Hydrated phases have been observed during corrosion of zircalloy at room temperature in the laboratory (Giupponi et al. 2012). The authors of this study carried out zircalloy oxidation in oxygen-helium mixtures to form a 6 µm porous oxide layer. This oxide layer has no tetragonal layer under as the one formed by water corrosion in reactor. The oxidized zircalloy was then irradiated with 1.5 MeV protons in humid air (6 and 50 mbar water partial pressures), leading to nitric acid formation. Probably the zircalloy was also corroded by nitric acid, because the surface layer of the oxide, analysed by XPS, was enriched in tin. The compounds proposed both for tin and zirconium are suggested based on inorganic chemistry textbooks and signal ratios on XPS spectra, from which it is difficult to confirm polynuclear complexes and even more difficult to determine water of hydration. Further, under the oxidizing conditions created by radiolysis, the authors suggest a reduction of Sn(IV) to Sn(II) by hydrogen, when radiolytic hydrogen should be inert at room temperature towards dissolved ions in solution. Thus, the conditions investigated in this study may be relevant for zircalloy corrosion in humid air in the presence of proton radiolysis and nitric acid formation, but not for the state of zircalloy cladding present in the dried canister.

On the other hand, it is reasonable to consider that the outer layer of the crystalline monoclinic ZrO_2(c) in contact with water at near neutral pH releases Zr(IV) ions in water and reaches with time a solubility equilibrium. Given the strong tendency to hydrolyse of Zr(IV) ions, they will be in the form of fully hydrolysed $Zr(OH)_4$(aq) ions at solutions of pH > 4 (Brown et al. 2005). This is the reason why at the surface of crystalline ZrO_2(c), a layer of a few atomic layers of hydrated oxide is formed, through the fixation at the surface of $Zr(OH)_4$ ions, which poly-condense one or two -OH groups with -OH groups at the surface to form Zr-O-Zr bonds, but still contain an undetermined number of -OH groups. The situation is the same as for ThO_2(cr) or UO_2(cr), which solubility at near neutral pH is determined by this hydrated oxide layer (Guillamont et al. 2003) generally denoted $UO_2 \cdot xH_2O$. This layer is extremely thin and it has not been able to detect with any method, but it is quite common for oxides of ions with strong hydrolysis and very low solubilities ($\sim 10^{-9}$ M), as is the case of zirconium oxide.

When ZrO_2(s) formed during corrosion in reactor is in contact with water e.g. in Clab, a solubility equilibrium is established between the oxide and water. At near neutral pH, zirconium (IV) ion is completely hydrolysed in solution and exists only as $Zr(OH)_4$(aq). It is very probable that similarly to the crystalline actinide oxide phases AnO_2(s), a layer of $ZrO_2 \cdot xH_2O$ is the one that determines the very low solubility of ZrO_2(s), which is equally low as that of UO_2(s) ($\sim 10^{-9}$ M). Anyhow, such layers are only a few atom layers thick, given the extremely low solubility of the amorphous phase. No direct detection of this layer has been possible, but water adsorption studies on ZrO_2(s) seem to confirm its presence.

Support for this hypothesis comes from studies which have measured water adsorption on ZrO_2(cr), claiming a few layers of non-reversibly adsorbed water, and denoted as chemisorbed water. Holmes et al. (1974) determined the adsorption of N_2, Ar and water on a sample of monoclinic ZrO_2 with BET surface area of 23.8 m^2/g as measured by adsorption of N_2 and Ar. The weight loss of the sample between 25 °C and 500 °C, in vacuum, was equivalent to 2,3 monolayers of chemisorbed water. The irreversible adsorption of water caused a 20 % decrease in the specific surface area as measured by Ar and N_2 adsorption. During the adsorption-desorption cycle of water, the chemisorption capacity of water was estimated as 4.8 mg/g irreversibly adsorbed water, i.e. 0.27 mg/m^2 by calculating with the reduced surface obtained after the first water contact. In marked contrast with the complex and slow kinetics of water adsorption-desorption at 25 °C, it was relatively easy to obtain reversible isotherms at 300 °C and 400 °C, a behaviour that the authors find similar to their study of ThO_2(c) (Gammage et al. 1970). Finally, they attribute the large quantity of irreversibly adsorbed water and the complex kinetics of adsorption to the formation of a hydrogen bonded network of molecular water on top of the surface hydroxyls. Maslar et al. (2001) carried out Raman spectroscopy on in-situ corroded Zr-Nd alloy in water at various temperatures and observed that monoclinic ZrO_2 features generally exhibit low intensities and broad line shapes, indicating that although the corrosion film thickness and/or crystallinity is increasing with exposure time and temperature, the corrosion layer is relatively thin and/or disordered.

Petrik et al. (2001) have carried out TPD (Temperature Programmed Desorption) of water multilayers from ZrO_2 powder and observe two broad peaks from chemisorbed water release. They estimate 8 molecules chemisorbed water per nm^2, out of which 4 are released at 27–200 °C and 4 in the interval 200–500 °C. This means that there are 8×10^{18} molecules/m^2 of oxide or $8 \times 10^{18}/6 \times 10^{23} = 1.33 \times 10^{-5}$ mol water/m^2 or 0.24 mg/m^2 chemisorbed water. This is in good agreement with the value 0.27 mg/m^2 from Holmes et al. (1974).

Recently, the report of Bryan et al. (2019) became available. They use the data of Holmes et al. (1974) to estimate the amount of chemisorbed water on zircalloy.

In any case, the chemisorbed water on zircalloy will not contribute to the relative humidity inside a sealed KBS-3 canister, since it starts to be released at temperatures which are never achieved in the canister. It contributes in the production of radiolysis products with quite different yields as compared to the radiolysis of free water (Petrik et al. 2001), with much higher yields of hydrogen production and almost complete absence of oxidants. By using the surface area of zircalloy in a PWR or BWR fuel assembly as reported in Bryan et al. (2019), the amount of chemisorbed water can then be estimated.

The report of Bryan et al. (2019) contains also data for the surface area of all components in a BWR or PWR fuel assembly. They state that in modern assemblies all assembly hardware is made of zircalloy (they state that some earlier assemblies had stainless steel hardware, but this seems still to be the case in Sweden) so this assumption is used for one version below, while in the other version the top and bottom nozzle in PWR assemblies and top and bottom tie plates in a BWR assembly are assumed to be made of stainless steel. As discussed above, chemisorbed water on zircalloy surfaces is ~0.25 mg/m^2 based on the data of Holmes et al. (1974) and Petrik et al. (2001), while the sum of physisorbed and chemisorbed water is 3 mg/m^2 based on the data of Holmes et al. (1974) and Hall et al. (1992). For stainless steel, the data on physisorption of water on 316 SS from Manaf et al. (2019) and Subhi et al. (2015), which report 60 mg/m^2, are considered preliminarily, but estimations will be made also with data for physisorption of water on iron or nickel from Lee and Staehle (1997). The amount of adsorbed water in the fuel assemblies is estimated as follows:

a) PWR assembly, all surface zircalloy: Total surface 43.52 m^2 (Bryan et al. 2019), amount of physisorbed and chemisorbed water 43.52 × 3 mg/m^2= 130.6 mg. For four assemblies in a canister, the total amount of water adsorbed on zircalloy will be 522 mg, or 0.52 g. If the top and bottom nozzle are made of stainless steel, the amount of physisorbed water in SS is 0.588 m^2 × 60 mg/m^2 = 35.3 mg by using surface area from Bryan et al. (2019) and water physisorption data of Manaf et al. (2019) and Subhi et al. (2015). With the same surface area, but with data of Lee and Staehle (1997) the physisorbed water on stainless steel is 0.588 m^2 × 2.2 mg/m^2= 1.3 mg. Thus, the total amount of physisorbed and chemisorbed water in a PWR fuel assembly with top and bottom nozzle made of stainless steel is 42.93 m^2 × 3 mg/m^2 = 128.8 mg on zircalloy and 1.3–35.3 mg on stainless steel. The higher value for physisorbed water on stainless steel and the variant of the PWR assembly with top and bottom nozzle made of stainless steel will be used further. The amount of physisorbed and chemisorbed water in such an assembly is 128.8 mg +35.3 mg= 164 mg. For four assemblies in a canister the amount of water adsorbed on the assembly surfaces is 164 × 4 = 656 mg or 0.66 g.

b) BWR assembly, all surface zircalloy: Total surface 17.39 m^2 (Bryan et al. 2019), amount of water adsorbed on zircalloy: 17.39 m^2 × 3 mg/m^2 = 52.2 mg. In 12 assemblies of a canister load, the amount of water adsorbed on zircalloy will be 12 × 52.2 = 626 mg or 0.63 g. When the top and bottom tie plates are made of stainless steel and by using only the higher data on physisorbed water on stainless steel by Manaf et al. (2019) and Subhi et al. (2015), the amount of physisorbed water on the steel will be 0.367 m^2 × 60 mg/m^2 = 22 mg. By summing this with the amount of water adsorbed on the zircalloy parts (17.02 m^2 × 3 mg/m^2 = 51.1 mg) it results in a total amount of adsorbed water in a BWR assembly of 51.1 + 22 = 73.1 mg. In the 12 BWR fuel assemblies of a canister load, the total amount of adsorbed water will be 876,8 mg or 0.88 g.

For more precise and relevant estimations here, better data for water adsorption on stainless steel (both studies on stainless steel report the same 4 weight increase data, even though published with 4 years difference and appear in general not reliable) are needed.

In the following, the amount of physisorbed and chemisorbed water in a canister without damaged fuel rods will be estimated from data measured at high (90 to 100 % RH) as:

BWR canister: 74 mg at the copper shell + 86 mg at the insert + 876.8 mg at the 12 fuel assemblies = 1036.8 mg or **1.04** g water.

PWR canister: 74 mg at the copper shell + 42 mg at the insert + 656 mg at the 4 assemblies = 772 mg or **0.77 g** water.

3.2 Canister with one rod that has an undetected cladding breach

The majority of fuel cladding breaches occur in the nuclear reactor, and mechanical damage (fretting) dominates (Olander 2009). During storage in the Clab, none of the factors that cause fuel cladding breaching does exist (fretting, water chemistry, hydrogen embrittlement, pellet-cladding interaction). In the SKB case all damaged fuel rods in the nuclear power plants have already been dried and packed in carbon steel containers with a stainless steel overpack in the Studsvik case, or in stainless steel Quivers by Westinghouse. The only damaged unprotected fuel rods are the ones actually in Clab. Damaged fuel rods expected to result from the future operation of the nuclear power plants in Sweden are assumed to be placed in steel containers before being sent to Clab (Evins and Hedin 2020).

As a first alternative it will be considered here that the known damaged fuel rods in Clab will be dried and stored in corresponding Quivers (Evins and Hedin 2020) and the only damaged fuel rods are those that have caused a fission gas release during storage in Clab, as measured at the detector in the ventilation system. There are several fuel transports that have shown higher than background ^{137}Cs and ^{134}Cs levels, but no detection of ^{85}Kr has been possible, even though their gas content has been analysed with a ^{85}Kr detector. Work is in progress to investigate closer all the cases and compare with Cs measurements at the nuclear power plants before transport of the fuel to Clab, in order to rule out Cs-contamination in the reactor by the presence of a damaged fuel rod in the same reactor load.

There are in total 4 (or 6) cases when Kr-85 has been detected and to search for these rods would be costly and not simple. In any case, the breached fuel rods will very probably be detected in the drying station of the encapsulation plant. In this case, out of all the canisters sealed, there will be 4(6) canisters in which there is an undetected breached fuel rod. This number can be revised, in case more rods result breached in the drying station. Given the low number of breached undetected fuel rods as compared to the total number of rods, the probability to have two of them in the same canister load is quite low, so the following analysis is for one breached fuel rod per canister.

In the initial pessimistic estimation of the amount of water in the canister, it was assumed that 1 % of the fuel rods were damaged (12 in a BWR canister) and the amount of water in each was assumed 50 ml or 50 g.

In Table 3-1 (compiled mostly by D. Schrire, Vattenfall), it can be seen that the internal free volume in a fuel rod has been larger in the older designs (30–40 ml) and has decreased in the more modern designs (11–25 ml). In the beginning of life (in reactor), when damages in the cladding often occur, the free volume tends to be slightly higher than at start, because the interatomic distances in the fuel decrease with burnup (Kleykamp 1985, Spino and Papaioanu 2000), but later the free volume decreases because of fuel swelling and fission gas build-up. Anyhow, the maximum amount of unbound water in a fuel rod, for the types of fuels used in Sweden collected in Table 3-1, seems to be below 40 g.

In some investigations carried out with entire damaged fuel rods (Kohli et al. 1985, Peehs et al. 1986) which were dried in several steps during long periods of time, it is reported that the total amount of water collected from a breached rod indicates that the fuel rods were not completely water logged. The total amount of water collected from these early design breached fuel rods ranged between 4 and 11 g.

Table 3-1. Internal free volume in fuel rods of different designs, as measured through rod puncture. Results at Beginning of Life (BOL) are reported separately from these at Middle or End of Life (MOL/EOL).

Fuel assembly type	BOL free volume cm^3	MOL/EOL free volume cm^3	Burnup MWd/kgU	Reference
17 × 17 AFA		13	44	Studsvik NF(P)-89/25
17 × 17 HTP		11	60	Studsvik N-06/220
17 × 17 RFA-2		15,5	34	Studsvik N-14/443
17 × 17 RFA-2		13	58	
15 × 15 AFA		20		
15 × 15 AFA		18	63	Studsvik/N-08/080
15 × 15 AFA		20–21	51–53	Studsvik N-14/151
15 × 15 KWU		24	35	Studsvik NF(P)-87/26
15 × 15 KWU		21,5	42	Studsvik NF(P)- 89/14
Exxon 8 × 8		27.1	24	Jädernäs and Lindgren 2019
Exxon 8 × 8		28.3	32.8	Jädernäs and Lindgren 2019
Exxon 8 × 8		35–40	14–22	Studsvik NF(P)-83/12
Exxon 8 × 8 BA		36–38	36	Studsvik NF(P)-87/30
AA 8 × 8		32–35	12–22	Studsvik NF(P)-83/66
AA 8 × 8		32	37	Studsvik NF(P)-85/30
AA 8 × 8		29–30	37–39	Studsvik NF(P)-87/23
AA 8 × 8		28	43	Studsvik NF(P)-89/16
AA 8 × 8		32.1	18	Jädernäs and Lindgren 2019
AA 8 × 8		29.3	18	Jädernäs and Lindgren 2019
AA 8 × 8		30.5	23.1	Jädernäs and Lindgren 2019
AA 8 × 8		33.2	13.2	Jädernäs and Lindgren 2019
AA 8 × 8 BA		29–32	27–30	Studsvik NF(P)-85/35
AA 8 × 8 BA		29,5	38	Studsvik NF(P)-86/15
AA 8 × 8 BA		27	43	Studsvik NF(P)-86/27
AA SVEA-64?		34	9,5	Studsvik NF(P)-88/40
AA 8 × 8/SVEA-64?	29–31	27–29	34–38	Studsvik NF(P)-89/12
Svea 64		31	12,4	Studsvik/N-19/148
Atrium 10B		25	12	STUDSVIK/N-09/092
Atrium 10B		17,6	47	STUDSVIK/N-16/210
Atrium 10B		19	40	STUDSVIK/N-11/121
Atrium 10XM		22,5	38	STUDSVIK/N-16/207
Atrium 10XP		23	43	STUDSVIK/N-12/134

Other information comes from an analysis of the radionuclide releases in Clab basins where at least 197 damaged fuel rods are interim stored[4] The releases can be assigned to come from about 6 % of the total mass of the known damaged fuel rods in storage, indicating that only a small part of the damaged rod fuel is in contact with basin water.

Under the assumption that the damaged fuel rod has gone through an industrial drying procedure in the encapsulation plant, most of the free or unbound water (maximum 40 g) should have been removed. Anyhow, the issue of the non-complete drying of damaged fuel rods has been discussed in several recent works in connection with the dry storage of spent fuel (ASTM 2016, Jung et al. 2013, Shukla et al. 2019, Knight et al. 2018, Bryan et al. 2019).

[4] Spahiu K, Evins L Z, 2021. Bränsleupplösning från skadade bränslestavar under förvaring i Clabs bassänger. SKBdoc 1935629 ver. 1.0, Svensk Kärnbränslehantering AB. (In Swedish.) (Internal document.)

In the analysis of the residual water after drying (Jung et al. 2013), an estimation of the unbound water in liquid and gas (vapour) phase and of the chemisorbed water on zircalloy has been made as follows.

The amount of residual unbound water in liquid phase is based on data from Peehs et al. (1986), which reported the amount of water collected from a waterlogged breached SNF rod vacuum heated at 160 °C for 7 hours and at 200 °C for 24 hours to be 1.9 to 3.8 ml (3 whole rods were tested). During 2 months of storage at 400 °C following drying, an additional 0.5 to 4.1 ml of water was collected. Similar observations were reported by Kohli et al. (1985) for a moisture release experiment of a water-logged BWR fuel rod. Two fuel rods were placed in separate chambers and water was extracted first by vacuum for 1 h collecting 3 ml from one rod and 2 ml from the other. Then holes were drilled in the plenum, the rods were heated to 100 °C and, by applying vacuum, an additional 7 ml respectively 2 ml water were collected from each rod, bringing the total amount of water released to 10 and 5 ml. After this initial drying, the rods were maintained at 325 °C for 2100 hours (almost 3 months) during which an additional 1 ml and 1.5 ml of water was released respectively.

Jung et al. (2013) use the data of these experiments to estimate the amount of residual water in a CASTOR V/21 cask for dry storage of spent fuel, housing 21 Westinghouse 15 × 15 assemblies and assuming that 50 of the 5 000 rods are breached. This amount is estimated as 200 ml, i.e. 50 rods × 4 ml = 200 ml.

Jung et al. (2013) state: *"Unbound liquid water can exist at capillary pressures in pores, cracks, and spaces in crud and sludge, in thin wetted surface films on wetted components; and in breached rods that have become waterlogged in the SNF pool. Based on the pressure-temperature phase equilibrium diagram of water, the mass of water existing in capillary state will generally be considered less than vapour phase water contained elsewhere in the canister".*

The amount of the water in the gas phase is estimated from the ideal gas law for a pressure of 3 torr achieved during drying and results in 0.34 mol (6 g) for a cask void volume of 2.1 m^3.

For physisorbed water they state that it can be dried easily during the vacuuming process, while for chemisorbed water they discuss mainly the case of zirconium hydroxides, by using analogies with aluminium hydroxides. They assume that a hydrated zirconium $ZrO(OH)_2$ with a thickness of 10 µm may form from the oxide present from reactor discharge or during pool storage. As references for this claim they give Giupponi et al. (2012), discussed in Section 3.1, and Powers and Gray (1973), which have studied the dehydration of a hydrated zirconium oxychloride salt ($ZrOCl_2 \times 8H_2O$), prepared from recrystallisation of $ZrCl_4$ in 1 M HCl, and mistakenly named zirconium oxide in Jung et al. (2013). From this and a density of 2 g/cm^3 for the hydrated oxide $ZrO(OH)_2$, they calculate 85 moles of chemisorbed water (1 530 g) in 600 m^2 of zircalloy cladding in their cask. They accept that there are no data on the quantity of the chemisorbed water on zirconium oxide, but state also that a quantitative uncertainty analysis is out of the scope of their report. Based on this analysis, they assume a total amount of residual water for the Castor V21 cask between 5.5 mol (100 g) and 55 mol (1 000 g). This is the reason why quite some effort was used in this report to discuss chemisorbed water on zirconium oxide in the previous section.

In another report published later concerning also consequence analysis of the effect of residual water in a dry storage cask (Shukla et al. 2019) it is stated that findings from recent DOE projects show that residual water well above the 0.4 mol (7.2 g), assumed for the 3 Torr rebound pressure and the volume of the cask, may remain in a SNF canister following prototypic drying. They have improved and expanded the model of Jung et al. (2013) with improved sub-models for water radiolysis, cladding oxidation and fuel oxidation. In the estimation of the amount of residual water in a canister they refer to the recent work of Knight et al. (2018) and a report by Bryan et al. (2019). The risk of ice formation during vacuum drying is mentioned based on the work of Knight et al. (2018) and is considered one of the main reasons of the residual water in the canister cavity. The report of Bryan et al. (2019) discusses work carried out in the high burnup cask demonstration project, which shows the presence of 100 g residual water in a canister cavity. For this reason, it is assumed that 5.5 moles up to 10 moles of water (100–180 g) are present in the dry fuel storage canister cavity. The upper limit takes into account also uncertainties associated with logged water in failed fuel rods and bound water with other assembly hardware.

The risk of ice formation exists also during fuel drying in the encapsulation plant, with the difference that the fuel assemblies will be transferred to the canister insert and ice formation e.g. at the bottom of the drying cask will not end up in the disposal canister. On the other hand, ice formation during drying of waterlogged fuel rods will result in residual water in the disposal canister. It seems therefore reasonable to assume that 4 ml water, associated with the incomplete drying of a damaged fuel rod will contribute in the residual water in the canister cavity. Besides this, there will be 0.77–1.04 g water from physisorbed water in the canister insert and fuel elements, see Section 3.1. In a KBS-3 canister with one breached and dried fuel rod, the amount of residual water is expected to be 0.77–1.04 g physisorbed water, and ~4 g in the not completely dried fuel rod.

The amount of chemisorbed water in the case of a damaged fuel rod includes also chemisorbed water in the oxidized uranium phases such as hydrated schoepite $UO_3 \cdot xH_2O$, $x < 2$ or hydrated studtite $UO_4 \cdot 4\ H_2O$, which may form during the corrosion of the damaged fuel rods in the reactor pools or in Clab. According to data reported in ASTM (2016) all these hydrated compounds decompose at about 150 °C and if a higher temperature is applied during drying, only $UO_2(OH)_2$ will be present in the damaged fuel rod, because it decomposes to UO_3 and H_2O above 250 °C. It is possible that this amount of water is already included in the 4 g of residual water calculated for a dried fuel rod, because much higher temperatures than 250 °C were used during drying. Anyhow, for the fuel rods dried under vacuum and no temperature increase an approximate estimation of this amount of water can be made as follows:

There is a large SKB database with fuel leaching under oxidizing conditions where the rate of fuel dissolution in the presence of air was estimated as 10^{-4}–10^{-5}/year. By using the upper limit and a mass of fuel in a fuel rod 198 kg fuel BWR assembly / 96 rods = 2.062 kg UO_2(s)/rod, and a leaching time of 30 years (most of the fuels were dried in 2015–2018), the mass of converted UO_2 results as 6.186 g or 0.023 mol. This amount of uranium will here be assumed to have been completely precipitated as $UO_4.4H_2O$ or $UO_2(OH)_2.H_2O$ and no uranium has dissolved in the pools. Each mol of the first compound contains 4 mol of chemisorbed water, each mol of the second contains 2 mol of chemisorbed water. This means that the maximal amount of chemisorbed water in a fuel rod will be $4 \times 0.023 = 0.091$ mol water or 1.65 g water. Tetra-hydrated studtite decomposes to di-hydrated studtite at relatively low temperatures 25–100 °C (ASTM 2016) and this would lower the amount of chemisorbed water to 0.83 g per fuel rod. Anyhow, in the following the higher amount of chemisorbed water is considered, i.e. in a not completely dried fuel rod it will be assumed that 4 g + 1.65 g = 5.65 g water is present. Considering also the 0.77–1.04 g of water adsorbed in the copper shell, canister insert and fuel assemblies, the total amount of water in a canister with one damaged fuel rod is estimated to be 6.4 g–6.7 g.

The consequences of 6.4 to 6.7 g residual water in a KBS-3 canister have been modelled by Hernshaw and Spahiu (2021) in a dedicated calculation case. If corrosion is not considered, the radiolysis produces 26 g HNO_3, 0.15 mol O_2 and 0.08 mol H_2O_2. The produced nitric acid is only half of that produced in presence of about 90 times more water (600 g).

When accounting for iron corrosion, independently of the oxic iron corrosion rate, all oxidants drop to negligible levels ($< 10^{-15}$ mol). One of the major advantages of a canister load with such a low amount of residual water is that even in the presence of 10 % air there is almost no ammonia formed ($< 10^{-22}$ mol), while with 1 % air the produced ammonia drops to extremely low levels (1.5×10^{-44} mol). This is because in this case much lower amounts of hydrogen are produced by the anoxic corrosion of iron due to the consumption of the small amount of water mostly during oxic corrosion.

3.3 Canister with a known failed fuel rod and one unknown failed fuel rod

There are a total number of 251 known or suspected damaged fuel rods in Clab and it can be considered reasonable to distribute them in different canister loads during the fuel drying in the encapsulation plant. This implies that fuel rod handling, which is not possible presently at Clab, has become possible. Besides this known damaged fuel rod, it may happen that one of the unknown 4–6 fuel rods damaged during storage in Clab is also packed in the same canister. The probability is low that one of the 6 unknown damaged rods will be in one of the 251 canisters which contain also one known damaged

rod, but not zero, and concerns only 4–6 canisters in total, out of all the sealed canisters. The amounts of physisorbed and chemisorbed water are expected to be the same as in the previous case, except for the residual and chemisorbed water in damaged fuel rods, which is twice as much, i.e. $5.65 \times 2 = 11.3$ g. Thus, the total amount of water in this type of canister will be 12.3 g water. The time to consume this amount of water considering only anoxic iron corrosion with a corrosion rate of 3 μm/year is 12.7 days. Even in this case, most of this small amount of water will be consumed by oxic iron corrosion and the production of hydrogen will be very limited, similar to the case with one fuel rod discussed in the previous section. This case was not modelled specifically, given its low probability of occurrence, but the production of radiolytic oxidants and ammonia in the presence of iron corrosion are expected to be only slightly higher than in the case with one damaged fuel rod and certainly much lower than the case discussed in the next section.

3.4 Other potential cases with more than 2 failed fuel rods

There are several containers for damaged fuel rods at Clab and the case of the one with the largest number of damaged fuel rods (43) was selected as a calculation case in Henshaw and Spahiu (2021). The amount of residual water in this type of canister is estimated as: 43×5.65 g/rod + 1 g water sorbed in the canister material = 244 g. As in the rest of the work, the production of radiolytic species neglecting iron corrosion was first carried out. The radiolysis produces 55.4 g HNO_3, 1.81 moles H_2O_2 and almost 3 moles H_2. The discussion in the first part of the report that 600 g water is not probable seems less relevant when considering that 244 g water leads to production of slightly more nitric acid than 600 g water, but the production of H_2O_2 is lower.

Accounting for iron corrosion results in very low nitric acid production (0.16 mg) and other oxidants, H_2O_2 or O_2 ($< 10^{-12}$ mol). When using a lower oxic corrosion rate, slightly more HNO_3 is produced, but the total amount is anyhow low (0.27 mg). The time to consume this amount of water through only anoxic iron corrosion would be ~252 days and it is slightly shorter when considering the initial phase of oxic iron corrosion. When reducing conditions are established in the canister interior, the production of ammonia starts and reaches 1.73 moles. Anyhow, there is no time period when ammonia and water coexist in this case, water is already consumed when ammonia production starts.

By lowering the presence of air to 1 %, the amount of nitric acid formed by this amount of water when neglecting iron corrosion drops to 4.1 g (from 55.4 g with 10 % air) and the production of other oxidants is: H_2O_2 1.52 mol and O_2 0.1 mol.

By considering iron corrosion for 244 g water and 1 % air, the production of nitric acid drops to 13 ng HNO_3, while this of the other oxidants is negligible ($< 10^{-16}$ mol).

It seems that even this amount of residual water, especially when lowering the air content to 1 %, has no large consequences in the canister atmosphere. This is based on the assumption that the fuel rods are dried by an industrial drying process (vacuum and high temperature or FGD) so that the estimation of residual water in a damaged fuel rod is valid.

The 197 known damaged fuel rods in Clab are either part of a fuel assembly or are stored in damaged rod containers with various numbers of failed rods[5]. Given that no fuel rod handling is possible at Clab presently, their potential loading in the canister will be discussed based on their actual number in assemblies or damaged rod containers.

There are 12 assemblies or containers, each with 1 damaged rod and in this case the amount of water in the canister load can be estimated as 6.7 g, while the consequences are as discussed in Section 3.2. If in the remaining undamaged fuel loaded in this canister there is an unknown damaged fuel rod, this converts to the case discussed in Section 3.3.

There is one assembly or container each with 2, 3, 5, 7, or 8 rods, two assemblies or containers with 6 or 10 damaged rods each, three assemblies with 4 damaged rods each, and besides the container with 43 damaged rods discussed previously in this section, there are 4 containers with 13, 15, 16 or

[5] Huuva E, 2021. Läckande bränsle i Clab bassänger. SKBdoc 1911213 ver. 1.0, Svensk Kärnbränslehantering AB. (In Swedish.) (Internal document.)

29 rods. If each of these assemblies or rod containers is loaded in one of the fuel positions and the remaining 11 positions are loaded with regular fuel, the estimated amount of residual water will be between 6.7 g (1 rod) and 244 g (43 rods). The production of nitric acid will be lower than 0.16 mg (< 13 ng for 1 % air) and this of the other oxidants H_2O_2 and O_2 lower than 10^{-12} mol, thus with no measurable consequences for the fuel or the canister materials.

3.5 Amount of residual water in Studsvik containers and Quivers

There are some remaining uncertainties about the amount of residual water in Quivers and Studsvik containers, even though they have all cleared a pressure rebound test and the internal atmosphere is pure inert gas. This residual water will affect only the fuel inside the same container, but not the copper canister or the fuel outside this container. If the residual water in a fuel rod is assumed equal to that of fuel submitted to standard fuel drying procedure before fuel transport, then residual water may amount to 4 g water /fuel rod as selected by Jung et al. (2013), based on the data of Peehs et al. (1986). It may also be that 5 g water/ fuel rod have to be assumed, as resulted from fuel rods transported at Studsvik from Germany (Karlsson et al. 2019). Given the large number of damaged fuel rods in one of these containers, substantial amounts of residual water may result this way.

Recent experimental data from the German Quiver project (Faber et al. 2020) show that the temperature at which fuel drying is carried out has a very large impact on the drying of water pockets in the fuel rod. They simulated these fuel pockets by connecting two reservoirs with a 50 cm long segment of a fuel rod, loaded water in the upper reservoir (simulating the fuel pocket) and measured water release under vacuum at various temperatures in the other. Their data indicate that at 35 °C the IAEA pressure rebound test (IAEA 2009, ASTM 2016) could be cleared, i.e. the pressure did not rise over 4 mbar when stopping the vacuum pump for 30 min. even though there was still water in the upper reservoir. At higher temperatures, even at 50 °C and 70 °C, the pressure raised over 4 mbar during the 30 min hold. This means that when performing fuel drying at 35 °C it is impossible to detect water pockets based on the pressure rebound test, making it thus difficult to quantify the amount of residual water in the damaged rods.

For a more detailed analysis of the consequences of residual water in Studsvik containers, the number of failed fuel rods placed in such a container, as well as the total surface area of the carbon steel part of the container are needed in order to estimate the amount of residual water, as well as the amount of water consumed by iron corrosion. In the case of Quivers made of stainless steel, the issue of residual water is probably more problematic, because the consumption of water by corrosion of the stainless steel is much slower than by carbon steel, thus radiolytic decomposition of water may be more extensive. On the other hand, the temperature in these canisters is expected to be lower, which will result in a much slower oxidation of only a small part of the damaged fuel rod (~3 cm on both sides of the defect (Einziger and Cook 1985)) by radiolytic oxygen.

3.6 Summary on the estimation of residual water in a sealed canister

The question that was posed in the beginning of this section was “How much water can be expected to be present in a sealed KBS-3 canister?”

In this section it was estimated that the total amount of physisorbed, chemisorbed and residual water in a canister containing one not completely dried failed fuel rod is 6.4–6.7 g. A thorough discussion of available data on chemisorption of water on zircalloy and on oxidized uranium compounds formed during interim storage of damaged fuel in ponds has been carried out and pessimistic values have been chosen. The amount of residual water in cases of canisters with more than one damaged fuel rod is evaluated based on these estimations. The modelling results for a canister loaded with a large number (43) of damaged rods have been carried out and are discussed, together with other potential canister loads with various numbers of damaged fuel rods (between 1 and 43).

It is necessary to obtain data on the residual water in the containers with dried damaged fuel (Quivers and Studsvik containers), in order to evaluate its consequences for the fuel oxidation.

4 Overall conclusions

This report explores potential effects of residual water and gases in a sealed KBS-3 canister. The purpose is to provide background information and support for decisions concerning requirements and acceptance criteria for the sealed canister. Two questions were posed: “Is 600 g water acceptable for the copper canister and for the fuel?” and “How much water can be expected to be present in a sealed KBS-3 canister?”

The first question relates to a hypothetical situation for the case of spent fuel, because the limit of 600 g water was established when SKB had not developed the approach of drying and packaging damaged fuel rods in hermetic containers under inert gas atmosphere. Besides being improbable to have so much water, since it originates mainly from damaged fuel rods, it is difficult to discuss its effects without knowing how much bare fuel surface is available for oxidation by the radiolytic oxygen produced. Anyhow, the recent modelling of the processes occurring inside the canister including radiolysis and iron corrosion makes it possible to answer the first question. The amounts of oxidants formed in the canister interior when considering radiolysis and iron corrosion is very small and becomes even lower for 1 % air. This means there are no consequences for exposed fuel surfaces, thus 600 g water is acceptable for the fuel.

The recent modelling results show also that when the oxygen of the air is consumed and reducing conditions are established in the canister interior, ammonia is produced by radiolysis of N_2 and H_2 mixtures at the levels of 1.3 mol for 10 % air and 0.13 mol for 1 % air. There is no period when water and ammonia coexist in the case of 1 % air, but a period of ~150 days of such coexistence in the case of 10 % air raises some reservations for this case, because ammonia can potentially lead to altered corrosion mechanisms of the canister materials. Thus, the consequences of 600 g water for the canister materials are dependent upon the amount of residual air allowed.

The second question has been answered as completely as possible based on published literature data, and the amounts of physisorbed water on the copper shell, canister insert and fuel assemblies have been evaluated, including the chemisorbed water on the zircalloy cladding. This amounts to 0.8–1 g water. If the known damaged fuel rods actually in Clab are packaged one per canister, the maximum amount of water in a canister is 6.7 g, including chemisorbed water on oxidized uranium compounds formed during pool storage of damaged rods. This amount of water in the canister gives rise to negligible amounts of oxidants and almost no ammonia in the canister.

Alternatives with a larger number of damaged and dried fuel rods (43) per canister have also been investigated. The production of HNO_3 is slightly higher than with the assumed 600 g water case discussed in the first part of the report. When considering iron corrosion, extremely small amounts of oxidants are produced. There is no doubt that iron corrosion will occur simultaneously with radiolysis in the canister, the issue is only at which rates. The rates chosen in the modelling work are well founded on experimental data and the real rates are expected to be even higher than those used in the modelling.

All the modelling results indicate a substantial decrease of all oxidants and ammonia in the canister atmosphere when the air content is lowered to 1 %.

References

SKB's (Svensk Kärnbränslehantering AB) publications can be found at www.skb.com/publications.
SKBdoc documents will be submitted upon request to document@skb.se.

Alcock C B, Jakob K T, Zador S, 1976. Zirconium: Physico-chemical properties of its compounds and alloys: Thermochemical properties. Atomic Energy Review Special issue 6.

Arkhipov O P, Verkhovskaya A O, Kabakchi S A, Ermakov A N, 2007. Development and verification of a mathematical model of the radiolysis of water vapor. Atomic Energy 103, 870–874.

ASTM, 2008. ASTM C1553–08: Standard guide for drying behavior of spent nuclear fuel. West Conshohocken, PA: ASTM International.

ASTM, 2016. ASTM C1553–16: Standard guide for drying behavior of spent nuclear fuel. West Conshohocken, PA: ASTM International.

Bartels D M, Henshaw J, Sims H E, 2013. Modeling the critical hydrogen concentration in the AECL test reactor. Radiation Physics and Chemistry 82, 16–24.

Brown P, Curti E, Grambow B, Ekberg C, 2005. Chemical thermodynamics of zirconium. Paris: OECD/NEA.

Bryan C R, Durbin S G, Lindgren E, Ilgen A G, Montoya T J, Dewers T, Fascitelli D, 2019. SNL contribution: Consequence analysis for moisture remaining in dry storage canisters after drying. Report SAND2019-8532 R, Sandia National Laboratory, Albuquerque, New Mexico.

Cera E, Bruno J, Duro L, Eriksen T, 2006. Experimental determination and chemical modelling of radiolytic processes at the spent fuel/water interface. Long contact time experiments. SKB TR-06-07, Svensk Kärnbränslehantering AB.

Cui D, Ekeroth E, Fors P, Spahiu K, 2008. Surface mediated processes in the interaction of spent fuel or alpha doped UO_2 with H_2. MRS Online Proceedings Library 1104, 305. doi:10.1557/PROC-1104-NN03-05

Dante J F, Kelly R G, 1993. The evolution of the adsorbed solution layer during atmospheric corrosion and its effects on the corrosion rate of copper. Journal of The Electrochemical Society 140, 1890–1897.

Dellongueville M, Issard H, Zechandru A, Leoni E, 2013. Fuel behavior in transport and dry storage, a key issue for the management of used nuclear fuel: An industry view. In Procedings of LWR Fuel Performance Meeting (Top Fuel 2013), Charlotte, NC, 15–19 September, 557–563.

Einziger R E, Cook J A, 1985. Behavior of breached light water reactor spent fuel rods in air and inert atmospheres at 229 °C. Nuclear Technology 69, 55–71.

Einziger R E, Strain R V, 1986. Behavior of breached pressurized water reactor spent fuel rods in an air atmosphere between 250 and 360 °C. Nuclear Technology 75, 82–95.

Einziger R E, Thomas L E, Buchanan H C, Stout R B, 1992. Oxidation of spent fuel in air at 175 to 195 °C. Journal of Nuclear Materials 190, 53–60.

Eriksen T E, Jonsson M, Merino H, 2008. Modelling of time resolved and long contact time dissolution studies of spent nuclear fuel in 10 mM carbonate solution – A comparison between two different models and experimental data. Journal of Nuclear Materials 375, 331–339.

Evins L Z, Hedin A, 2020. Failed fuel in special containers: potential contribution to risk calculated in the post-closure safety for the spent nuclear fuel repository. SKBdoc 1872793 ver 1.0, Svensk Kärnbränslehantering AB.

Faber W, Verwerft M, Pakarinen J, Rirschl C, 2020. The scientific backing of the German Quiver project. Atw. Internationale Zeitschrift für Kernenergie 65, 561–570.

Gammage R B, Fuller E L, Holmes H F, 1970. Gravimetric adsorption studies of thorium oxide. V. Water adsorption between 25 and 500°. The Journal of Physcal Chemistry 74, 4276–4280.

Garvie R C, 1965. The occurrence of metastable tetragonal zirconia as a crystallite size effect. The Journal of Physical Chemistry 69, 1238–1243.

Giupponi C, Millard-Pinard N, Bererd N, Serris E, Pijolat M, Peres V, Wasselin-Turpin V, 2012. Modification of oxidized Zircaloy-4 surface in contact with radiolysed wet air. Nuclear Instruments and Methods in Physics Research Section B: Beam Interactions with Materials and Atoms 272, 222–226.

Gras J-M, 2014. State of the art of ^{14}C in Zircaloy and Zr alloys – ^{14}C release from zirconium alloy hulls. Deliverable D 3.1 of the European Project CAST. European Commission.

Guillamont R, Fanghänel T, Grenthe I, Neck V, Palmer D, Rand M H, 2003. Chemical thermodynamics. Vol 5. Update on the chemical thermodynamics of uranium, neptunium, plutonium, americium and technetium. Amsterdam: Elsevier.

Hall P G, Langran-Goldsmith H, 1992. Inelastic incoherent neutron scattering from titanium and zirconium dioxides: Lattice phonon modes and librations of adsorbed water. Journal of Physical Chemistry 96, 867–870.

Hanson B D, Daniel R C, Casella A M, Wittman R S, Wu W, MacFarlan P J, Shimskey R W, 2008. Fuel-In-Air. FY07 Summary report. Report PNNL-17275, Pacific Northwest National Laboratory, Richland, WA.

Hanson B D, 1998. The burnup dependence of light water reactor spent fuel oxidation. Report PNL–11929, Pacific Northwest National Laboratory, Richland, WA.

Haschke J M, Allen T H, Stakebake J L, 1996. Reaction kinetics of plutonium with oxygen, water and humid air: moisture enhancement of the corrosion rate. Journal of Alloys and Compounds 243, 23–35.

Henderson M A, 1992. The interaction of water with solid surfaces: fundamental aspects revisited. Surface Science Reports 46, 1–308.

Henshaw J, 1994. Modelling of nitric acid production in the Advanced Cold Process Canister due to irradiation of moist air. SKB TR 94-15, Svensk Kärnbränslehantering AB.

Henshaw J, Spahiu K, 2021. Radiolysis calculations of air, argon and water mixtures in a KBS-3 canister. SKB TR-21-11, Svensk Kärnbränslehantering AB.

Henshaw J, Hoch A, Sharland S M, 1990. Further assessment studies of the Advanced Cold Process Canister. AEA-D&R Report 0060.

Holmes H F, Fuller E L, Gammage R A, 1972. Heats of immersion in the zirconium oxide–water system. The Journal of Physical Chemistry 76, 1497–1502.

Holmes H F, Fuller E L, Beh R A, 1974. Adsorption of argon, nitrogen and water vapour on zirconium oxide. Journal of Colloid and Interface Science 47, 365–371.

IAEA, 2009. Management of damaged spent nuclear fuel. Vienna: International Atomic Energy Agency. (IAEA Nuclear Energy Series NF-T-3.6)

Icenhour A S, Toth L M, Wham R M, Brunson R R, 2004. A simple kinetic model for the alpha radiolysis of water sorbed on NpO_2. Nuclear Technology 146, 206–209.

Johansson A J, Neretnieks I, 2014. Corrosion of the copper canister inside due to radiolysis of remaining water in the insert. SKBdoc 1419961 ver 1.0, Svensk Kärnbränslehantering AB.

Jonsson M, 2021. Impact of H_2 on the production of corrosive species in water vapor exposed to gamma radiation in canister for spent nuclear fuel. SKB R-21-14, Svensk Kärnbränslehantering AB.

Jung H, Shukla P, Ahn T, Tipton L, Das K, He X, Basu D, 2013. Extended storage and transportation: Evaluation of drying adequacy. Center for Nuclear Waste Regulatory Analysis (CNWRA), San Antonio, TX.

Jädernäs D, Lindgren H, 2019. Project Hoff-fission gas analysis of six O1 rods and one O2 rod. Studsvik Report Stusvik/N-19/148.

Kansa E J, Hanson B D, Stout R B, 1999. Grain size and burnup dependence of spent fuel oxidation: geological repository impact. In Wronkiewicz D J, Lee J H (eds). Scientific basis for nuclear waste management XXII: symposium held in Boston, Massachusetts, 30 November – 4 December 1998. Warrendale, PA: Materials Research Society. (Materials Research Society Symposium Proceedings 556), 455–462.

Karlsson J K-H, Puranen A, Tejland P, Pakarinen J, Johnson K, Askeljung C, Alvarez A-M, Benen A, Hüttman A, Lundberg S, 2019. Post-irradiation examination of KKB special fuel rods. In Proceedings of Global/Top Fuel, Seattle, WA, 22–26 September 2019, 344–353.

Kleykamp H, 1985. The chemical state of the fission products in oxide fuels. Journal of Nuclear Materials 131, 221–246.

Knight T, Faruk T, Khan J, Roberts E, Tulenko J, Tarbutton J, 2018. Experimental determination and modelling of used fuel drying by vacuum and gas circulation for dry casc storage. Final report. U.S. Department of Energy.

Knoll R W, Gilbert E R, 1987. Evaluation of cover gas impurities and their effects on the dry storage of LWR spent fuel. Report PNL-6365, Pacific Northwest Laboratory.

Kohli R, Stahl D, Pasupathi V, Johnson A B, Gilbert E R, 1985. The behavior of breached boiling water reactor fuel rods on long-term exposure to air and argon at 598 K. Nuclear Technology 69, 186–197.

Korzhavyi P A, Vitos L, Andersson D A, Johansson B, 2004. Oxidation of plutonium dioxide. Nature Materials 3, 225–228.

Lee S, Staehle R W, 1997. Adsorption of water on copper, nickel and iron. Corrosion 53, 33–42.

Leenaers A, Sannen L, Van den Berghe S, Verwerft M, 2003. Oxidation of spent UO_2 fuel stored in moist environment. Journal of Nuclear Materials 317, 226–233.

Li C, Olander D R, 1999. Steam radiolysis by alpha particle irradiation. Radiation Physics and Chemistry 54, 361–371.

Lilja C, 2012a. Inre övertryck i kapseln. SKBdoc 1333208 ver 2.0, Svensk Kärnbränslehantering AB. (In Swedish.)

Lilja C, 2012b. Svar på begäran om kompletteringar angående kapselfrågor. SKBdoc 1333256 ver 2.0, Svensk Kärnbränslehantering AB. (In Swedish.)

Manaf N D A, Fukuda K, Subhi Z A, Radzi M F M, 2019. Influence of surface roughness on the water adsorption on austenitic stainless steel. Tribology International 136, 75–81.

Maslar J E, Hurst W S, Bowers W J, Hendricks J H, 2001. In situ Raman spectroscopic investigation of zirconium-niobium alloy corrosion under hydrothermal conditions. Journal of Nuclear Materials 298, 239–247.

Miller L, Basu D, Das K, Mintz T, Pabalan R, Walter G, 2013. Overview of vacuum drying methods and factors affecting the quantity of residual water after drying – public version. CNWRA, San Antonio, Texas.

Olander D, 2009. Nuclear fuels – Present and future. Journal of Nuclear Materials 389, 1–22.

Olander D R, Wang W-E, Kim Y S, Li C Y, Lim S, Yagnik S K, 1997. Chemical processes in defective LWR fuel rods. Journal of Nuclear Materials 248, 214–219.

Olander D R, Kim Y S, Wang W-E, Yagnik S K, 1999. Steam oxidation of fuel in defective LWR rods. Journal of Nuclear Materials 270, 11–20.

Ollila K, Lindqvist K, 2003. Air oxidation tests with Gd-doped UO_2. Preliminary dissolution tests with pre-oxidized Gd-doped UO_{2+x}. Posiva 2003-08, Posiva Oy, Finland.

Pastina B, LaVerne J A, 2001. Effect of molecular hydrogen on hydrogen peroxide in water radiolysis. The Journal of Physical Chemistry A 105, 9316–9322.

Pastina B, Isabey J, Hickel B, 1999. The influence of water chemistry on the radiolysis of the primary coolant water in pressurized water reactors. Journal of Nuclear Materials 264, 309–318.

Peehs M, Bodelmann R, Fleisch J, 1986. Spent fuel dry storage performance in inert atmosphere. In Proceedings of the 3rd International Spent Fuel Storage Technology Symposium, Seattle, WA, 8–10 April 1986. Vienna: IAEA, S215–S230.

Petrik N G, Alexandrov A B, Vall A I, 2001. Interface energy transfer during gamma radiolysis of water on the surface of ZrO_2 and some other oxides. The Journal of Physical Chemistry B 105, 5935–5944.

Powers D A, Gray H B, 1973. Characterization of the thermal dehydration of zirconium oxide halide octahydrates. Inorganic Chemistry 12, 2721–2726.

Puranen A, Barreiro A, Evins L Z, Spahiu K, 2017. Spent fuel leaching in the presence of corroding iron. MRS Advances 2, 681–686.

Rafalskiy R P, Alekseyev V A, Ananyeva L A, 1979. Phase-composition of synthetic and natural uranium oxides. Geokhimiya (Geochemistry) 11, 1601–1615. (In Russian.)

Roy C, David G, 1970. X-ray diffraction analysis of zirconia formed on zirconium and zircaloy-2. Journal of Nuclear Materials 37, 71–81.

Seo M, Sawamura I, Grasjo L, Haga Y, Sato N, 1990. Measurement of minute corrosion of copper thin film by a quartz crystal microbalance. Journal of the Society of Materials Science, Japan 39, 357–361.

Shukla P, Sindelar R, Lam P-S, 2019. Consequence analysis of residual water in a storage canister. Report SRNL-STI-2019-00495, Savannah River National Laboratory.

SKB, 2006. Long-term safety for KBS-3 repositories at Forsmark and Laxemar – a first evaluation. Main report of the SR-Can project. SKB TR-06-09, Svensk Kärnbränslehantering AB.

SKB, 2010a. Fuel and canister process report for the safety assessment SR-Site. SKB TR-10-46, Svensk Kärnbränslehantering AB.

SKB, 2010b. Design, production and initial state of the canister. SKB TR-10-14, Svensk Kärnbränslehantering AB.

SKB, 2010c. Data report for the safety assessment SR-Site. SKB TR-10-52, Svensk Kärnbränslehantering AB.

Smart N R, Rance A P, 2005. Effect of radiation on anaerobic corrosion of iron. SKB TR-05-05, Svensk Kärnbränslehantering AB.

Smart N R, Blackwood D J, Werme L, 2002. Anaerobic corrosion of carbon steel and cast iron in artificial groundwaters: Part 2 – Gas generation. Corrosion 58, 627–637.

Speller F, 1951. Corrosion, causes and prevention. 3rd ed. New York: McGraw-Hill.

Spino J, Papaioannou D, 2000. Lattice parameter changes associated with the rim-structure formation in high burn-up UO_2 fuels by micro X-ray diffraction. Journal of Nuclear Materials 281, 146–162.

Sridhar N, Cragnolino G A, Dunn D S, Manakhala H K, 1994. Review of degradation modes of alternate container designs and materials. Report CNWRA-94-010, Center for Nuclear Regulatory Analyses, San Antonio, TX.

SSM, 2012. Begäran om komplettering av ansökan om slutförvaring av använt kärnbränsle och kärnavfall – degraderingsprocesser för kapseln. Dnr SSM2011-2426-57, Swedish Radiation Safety Authority. (In Swedish.)

Subhi Z A, Fukuda K, Morita T, Suginama J, 2015. Quantitative estimation of adsorbed water layer on austenitic stainless steel. Tribology Online 10, 314–319.

Swanton S W, Baston G M N, Smart N R, 2015. Rates of steel corrosion and carbon-14 release from irradiated steels – state of the art review. Deliverable 2.1 of EU-project CAST. European Commission.

Taylor P, Wood D D, Duclos A M, Owen D G, 1989. Formation of uranium trioxide hydrates on UO_2 fuel in air-steam mixtures near 200 °C. Journal of Nuclear Materials 168, 70–75.

Taylor P, Wood D D, Owen D G, 1995. Microstructures of corrosion films on UO_2 oxidized in air-steam mixtures at 225 °C. Journal of Nuclear Materials 223, 316–320.

Thiel P A, Madey T E, 1987. The interaction of water with solid surfaces: fundamental aspects. Surface Science Reports 7, 211–385.

Thomas L E, Einziger R E, Woodley R E, 1989. Microstructural examination of oxidized spent PWR fuel by transmission electron microscopy. Journal of Nuclear Materials 166, 243–251.

Thomas L E, Einziger R E, Buchanan H C, 1993. Effect of fission products on air oxidation of LWR spent fuel. Journal of Nuclear Materials 201, 310–319.

Tosan J-L, 1991. Eude de l'hydrolyse de solutions d'oxychlorure de zirconium. Caractérisation des espèces en solution et des précipités gélatineux. Relation avec la nature de la zircone formée par pyrolyse, Ph. D. Thesis, Université Claude Bernard – Lyon I. (In French.)

Uhlig H H, Revie R W, 1985. Corrosion and corrosion control: an introduction to corrosion science and engineering. 3rd ed. New York: Wiley.

Wasywich K M, Hocking W H, Shoesmith D W, Taylor P, 1993. Differences in oxidation behavior of used CANDU fuel during prolonged storage in moisture-saturated air and dry air at 150 °C. Nuclear Technology 104, 309–329.

Arkitektkopia AB, Bromma, 2021

SKB is responsible for managing spent nuclear fuel and radioactive waste produced by the Swedish nuclear power plants such that man and the environment are protected in the near and distant future.

skb.se